Renewable and Sustainable Energy Reviews 28 (2013) 425–440

Contents lists available at ScienceDirect

Renewable and Sustainable Energy Reviews

journal homepage: www.elsevier.com/locate/rser

Researches and trends in membrane-based liquid desiccant air dehumidification

Si-Min Huang[a,b], Li-Zhi Zhang[a,b,*]

[a] Key Laboratory of Enhanced Heat Transfer and Energy Conservation of Education Ministry, School of Chemistry and Chemical Engineering, South China University of Technology, Guangzhou 510640, China

[b] State Key Laboratory of Subtropical Building Science, South China University of Technology, Guangzhou 510640, China

ARTICLE INFO

Article history:
Received 25 June 2012
Received in revised form
25 July 2013
Accepted 11 August 2013
Available online 30 August 2013

Keywords:
Membrane
Liquid desiccant
Air dehumidification
Cross-over problem
Membrane module

ABSTRACT

Membranes were used in combination to liquid desiccant air dehumidification to separate the liquid desiccant from the process air to prevent the problems of liquid droplets crossover. In this review, the developments in this relatively new technology were introduced. The membrane materials used for the selective permeation of moisture were described. The design of membrane modules, classified into parallel-plates type and hollow fiber type, were summarized. The key point under research was the modeling of conjugate heat and mass transfer in the membrane modules. Recent researches on the fundamental transport data in the membrane modules were collected and compared. They were useful for future component design and system optimum. At last, the system set up, and the applications of this new technology, were also introduced. It was discovered that the membrane-based liquid desiccant air dehumidification technology was an effective method to overcome the problem of solution droplets cross-over problems. Applications of this technology were promising after these years' accumulation of the insight into the dynamics of system performance and module behaviors.

Contents

1. Introduction

Many countries, especially in coastal areas, are in humid climates. In these regions, air dehumidification is a necessity otherwise human lives and production development will be seriously influenced by the humid climates. Without air dehumidification, occupants will feel uncomfortable and mildew would grow on building surfaces. Further, too high humidity would affect production safety and product quality.

* Corresponding author at: Key Laboratory of Enhanced Heat Transfer and Energy Conservation of Education Ministry, School of Chemistry and Chemical Engineering, South China University of Technology, Guangzhou 510640, China.
Tel./fax: +86 20 87114268.
E-mail address: lzzhang@scut.edu.cn (L.-Z. Zhang).

1364-0321/$ - see front matter
http://dx.doi.org/10.1016/j.rser.2013.08.005

Nomenclature

b/a	aspect ratios
C_D	total drag coefficient
COP	coefficient of performance
D	diffusivity (m^2/s)
D_h	hydrodynamic diameter (m)
D_f	fractal dimension
d	diameter (m)
f	friction factor
fRe	product of friction factor and Reynolds number
Gz	Graetz number
Nu	Nusselt number
Pr	Prandtl number
r	radius (m)
r_o/r_f	radius ratio
Re	Reynolds number
Sc	Schmidt number
Sh	Sherwood number
S_L	longitudinal pitch (m)
S_T	transverse pitch (m)
T	temperature (K)
Tcop	thermal coefficient of performance
u	velocity (m/s)

Greek letters

φ	packing fraction

Subscripts

a	air
ave	average (mean)
C	fully developed under naturally formed boundaries
f	free surface
H	uniform heat flux (mass flux) condition
i	inner
s	solution
T	uniform temperature (concentration) condition

In a word, air dehumidification has an important significance on people's quality of lives, as well as on the quality of production.

There were many air dehumidification methods, including cooling coils, liquid desiccant air dehumidification, solid desiccant dehumidification and electrochemical dehumidification [1,2]. Among them, liquid desiccant air dehumidification had gained much progress recently due to the coherent virtues of this technology [1,2]. It was highly efficient and it had no liquid water condensations. It could be regenerated by low-grade heat like solar energy. The regenerated concentrated solution could also be used as energy storage medium.

Packed beds, in which the liquid desiccant and the air stream exchanged heat and moisture in direct contact, were the traditional equipments to realize air dehumidification. However, since the liquid desiccant and the process air were in a direct contact, small liquid desiccant droplets might be carried over by the process air to indoor environment, which was rather harmful to occupant health, building structure and furniture. Crossover problems had become the major obstacles for liquid desiccant air dehumidification to be used widely in engineering applications.

To overcome the crossover problems, recently, selectively permeable membranes [3–6] had been combined to the liquid desiccant air dehumidification to form a new kind of liquid desiccant air dehumidification system-the so-called membrane-based liquid desiccant air dehumidification system. If powered by renewable energy sources, performance was rather high, in addition to no droplets cross over. A schematic of the system driven by solar heat was shown in Fig. 1.

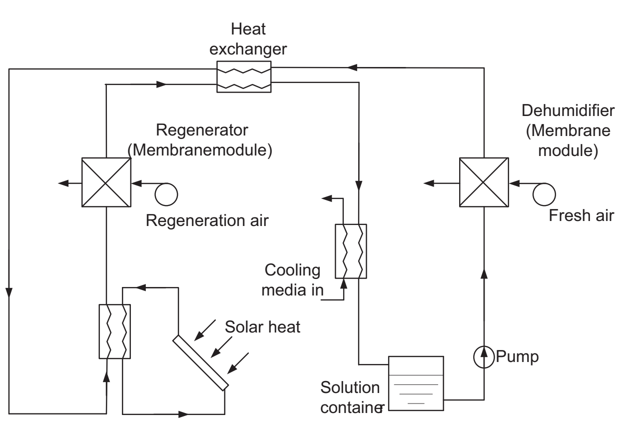


Fig. 1. Schematic of a membrane-based liquid desiccant air dehumidification system driven by solar energy [1].

The most obvious difference between this technology and a traditional one was that the traditional packing columns, either the dehumidifiers or the regenerators, were replaced by membrane-based modules. In these modules, semi-permeable membranes were used to separate the desiccant solution and the process air from each other. The membranes were able to prevent the solution from crossing over to the process air, while selectively permitting the transport of heat and moisture between the solution stream and the air stream.

Though this was a new technology, there were still many new developments in this area in the past 10 years. These developments were focused on three aspects: (1) Membrane materials; (2) Membrane modules to replace packed beds; (3) System design and applications. Mostly, the conjugate heat and mass transfer in the membrane modules had been given the top priority in a number of recent studies. This review gave a comprehensive analysis of these investigations.

2. Membrane materials for liquid desiccant air dehumidification

Polymer membranes had been used as the materials for liquid desiccant air dehumidification. There were many researches on the fabrications of moisture permeable membranes in South China University of Technology [3–6]. They were fabricated for heat and moisture recovery years ago, but extended to liquid desiccant air dehumidification recently.

The membrane modules were also usually called membrane contactors. In gas–liquid contactors, either hydrophobic microporous [3–5] or nonporous membranes [6] were commonly used. However, the microporous membranes had the potential risk of pore-wetting by the liquid desiccant. Therefore the unpredictable penetration of the liquid solution through the membrane should be seriously considered. In principle, the leakage of the liquid solution could be prevented by a careful adjustment of the trans-membrane pressure drop which was a function of the pore radius, the contact angle and the surface tension [7]. A too high pressure

at the air side might lead to a penetration of air into the liquid solution and vice versa at a too low pressure. For a given membrane material and its surface morphology, the wetting tendency was mainly affected by the surface tension of the applied solution. The higher the surface tension was, the lower the tendency towards pore-wetting was. Therefore it was suggested to increase the normally relatively low surface tension of organic absorbents by the addition of inorganic salts [8]. On the other hand, the presence of even trace amounts of surfactants might result in a considerable reduction of the breakthrough pressure [7]. The leakage often occurred only after a certain time of operation because the wetting was not only related to the surface tension. It might also be promoted by adhesion potentials of the hydrophobic membrane material, adsorption due to electrostatic interactions [8] or solute precipitation from the absorbent solution. The pore-wetting might also be facilitated by morphological changes of the membrane surface during operation which was observed for example with PP membranes used for CO_2 absorption in propylene carbonate [9].

These potential risks for leakage and hence caused restrictions in the operating conditions (i.e. type of liquid desiccant, pressure) in gas–liquid contactor processes (both in liquid desiccant dehumidification and in other liquid gas absorptions) could only be overcome reliably by applying nonporous membranes, which mainly contained the following types:

(1) The microporous membranes (PP, PE, PEI, PTFE, PVDF, etc.) coated with a dense silicone or gel layer [6,7,10,11].
(2) The different types of silicone coatings investigated at various absorption systems: volatile organics/silicone oil [12], CO_2/water or NaOH [13], etc.
(3) The homogeneous PDMS hollow fibers used in the absorption system CO_2/alkaline solution, carbonates [14].
(4) The microporous PTFE membranes coated with a dense layer of amorphous Teflon (Teflon AF), mentioned in absorption systems: water vapor or CO_2, SO_2, H_2S, NH_3/glycol or amines [15].

Above-mentioned membrane materials had been successfully employed for liquid desiccant air dehumidification. There are new membranes being developed.

3. Dehumidifiers

In order to realize a continuous operation, a complete liquid desiccant air dehumidification system included a dehumidifier, a regenerator, air and solution driven devices, and solution heating and cooling equipments. The low-grade energy sources such as solar energy, waste heat, could be used for liquid solution heating. The dehumidifier and the regenerator were ventilated with the process air and the regeneration air, respectively to realize air dehumidification and solution regeneration. In the dehumidifier, heat and moisture were exchanged between the liquid desiccant and the humid air. Latent heat of the air was removed. The air stream out from the dehumidifier was sent to an evaporative cooler for sensible heat exchange to adjust the air temperature. Then the supply air was sent to indoor spaces. It can be seen that it was a kind of independent air dehumidification process.

The dehumidifier and regenerator were the two key devices in the liquid desiccant air dehumidification system. In the dehumidifier, water vapor in the moist air was absorbed by the liquid desiccant to realize air dehumidification. Similarly, the water vapor in the liquid desiccant was released to the air to realize solution regeneration. The basic principles in the dehumidification process were similar to those in the regeneration process. The main difference was that the directions for water vapor transfer were in opposites. Therefore this review would only focus on dehumidifiers.

3.1. Packed columns for liquid desiccant air dehumidification

The traditional liquid desiccant air dehumidification devices used packed columns as dehumidifiers to realize heat and moisture exchange. Depending on whether there was a heat source in the dehumidifiers, they could be classified into adiabatic and internally cooled types [1,2].

3.1.1. Adiabatic type

The adiabatic dehumidifiers could be found in a wide range of industrial and residential applications. They could afford large air–desiccant contacting areas with relatively simple geometric configurations. Besides, its heat and mass transfer efficiency was relatively high. However, it had the potential drawback of imposing a large pressure drop on the process air when it flowed through the packing materials. Recent researches on this topic were focused on structural optimizations to have an improved performance.

In the adiabatic dehumidifier, there were no additional cooling sources to cool the liquid desiccant. Zurigat et al. [16] proposed a packed column dehumidifier with low packing density (77 m^2/m^3). Air dehumidification experiments were performed using triethylene-glycol (TEG) as desiccant under hot and humid conditions. Two different structured packings, wood and aluminum, were used. The results were compared to the Chung correlation [17], which over-predicted the effectiveness. Similarly, the Martin and Goswami correlation [18] failed to predict the effectiveness as well. A more accurate correlation was given in this study [16]. It was found that the moisture removal rate increased with increasing inlet TEG concentration, TEG flow rate and air flow rate. The rule held for both the wood and the

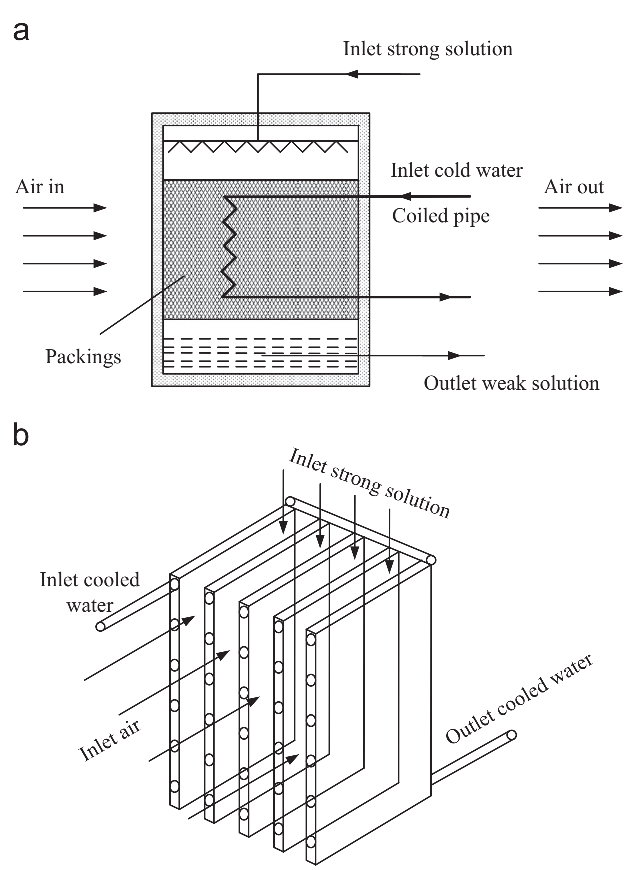


Fig. 2. Schematic diagram of internally cooled dehumidifiers. (a) Packing column type [1,2]; (b) spaced parallel plate type [24].

aluminum packings. Babakhani and Soleymani [19] presented a new analytical solution of heat and mass transfer processes in an adiabatic packed bed dehumidifier. Compared with numerical solution, the analytical solution had advantages in analyzing the parameters that affected the heat and mass transfer performances. Based on the analytical solution proposed in this paper, correlations of the dehumidification effectiveness and the condensation rate in the packed bed dehumidifier were analytically obtained and experimentally validated. Moon et al. [20] presented new mass transfer performance data of a cross-flow liquid desiccant dehumidification system using a structured packed tower. The structured packing consisted of cross-corrugated cellulose paper sheets with a specific surface area of 608 m^2/m^3. A new empirical correlation was developed for the dehumidification effectiveness. The effects of air and solution inlet conditions and flow rates on the system performance were also quantified. Zhang et al. [21] experimentally studied an adiabatic dehumidifier made by a 500 mm long and 270 mm wide transparent plastic rectangular parallelepiped. When the air velocities were ranging from 0.5 to 1.5 m/s, the mass transfer coefficient in the structured dehumidifier varied from 4.0 to 8.5 g/m^2 s. Gao et al. [22] experimentally investigated the heat and mass transfer between air and liquid desiccant in a structured dehumidifier packed by Celdek packings. The results showed that better performance could be obtained by increasing the width or height simultaneously. Longo and Gasparella [23] presented the experimental tests on the chemical dehumidification of air by a liquid desiccant in an absorption tower with random packing. The experimental tests showed that chemical dehumidification of air by liquid desiccants ensured consistent reduction in humidity ratios, which was suitable for the application in air conditioning or drying processes.

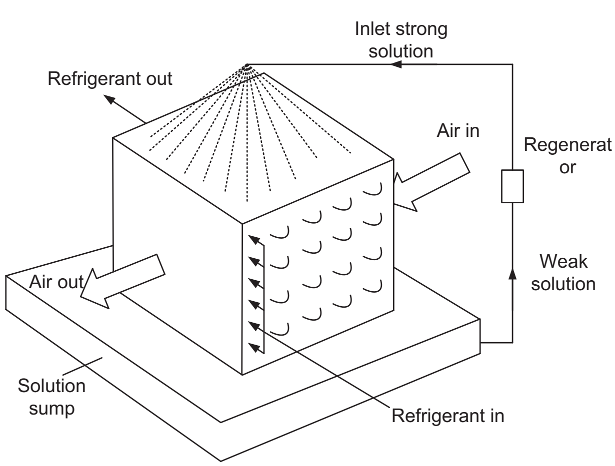


Fig. 3. Schematic of another internally cooled dehumidifier [25].

The aforementioned researches on adiabatic dehumidifiers [16–23] were mostly focused on structural optimizations. It is obvious that the performance of the dehumidifier can be enhanced by these researches. However, the increase of the performance is limited due to the temperature increase caused by the water vapor absorption. To address this problem, internally cooled type dehumidifier was employed.

3.1.2. Internally cooled type

In adiabatic dehumidifiers, an increase in temperature of liquid desiccant during the moisture removal process would exert an adverse impact on the performances, which in turn made both temperature and humidity control of the process air less effective. As a result, the internally cooled dehumidifiers using cooling coils to remove the heat generated from dehumidification might be a sound alternative. The absorption heat could be taken away by the cooling coils installed inside the dehumidifiers effectively. It was obvious that the liquid desiccant stream and the cooling stream should be separated strictly. Therefore the special devices in internally cooled dehumidifiers may, to some extent, increased the equipments requirement.

The apparatuses, as shown in Fig. 2(a) and (b), were two commonly used inner cooled dehumidifiers. As seen from Fig. 2(a), the cooling coils embedded in the packings were employed to remove the phase heat generated due to water vapor absorption by liquid desiccants. In the dehumidifier, the air and the solution through the packing materials were arranged to be cross flow. They could also be replaced by parallel and counter flow configurations. An outer insulation layer was wrapped on the dehumidifier to prevent heat transmission from the outside. However, the insertion of cooling coils into the packing materials made the installation more difficult. To realize an optimal humidity control, large mass flow rates of desiccant solution were required for such dehumidifiers. Yoon et al. [24] proposed another type of internally cooled dehumidifier, as depicted in Fig. 2(b). As seen, vertical plates were lined with equal spacings. Strong desiccant solution was uniformly distributed and it flowed down each plate along both sides of plates. The solution in falling film was cooled by the counter flow cooling water inside the plates. The parallel-plates could be replaced by corrugated plates to enlarge the air–desiccant contacting area and thus to enhance dehumidification. This type of dehumidifier was promising because the absorption heat released in one channel could be removed effectively by the cooling water in another neighboring channel.

Khan and Sulsona [25] chose a device shown in Fig. 3 as the dehumidifier. As seen, the absorber was essentially a conventional

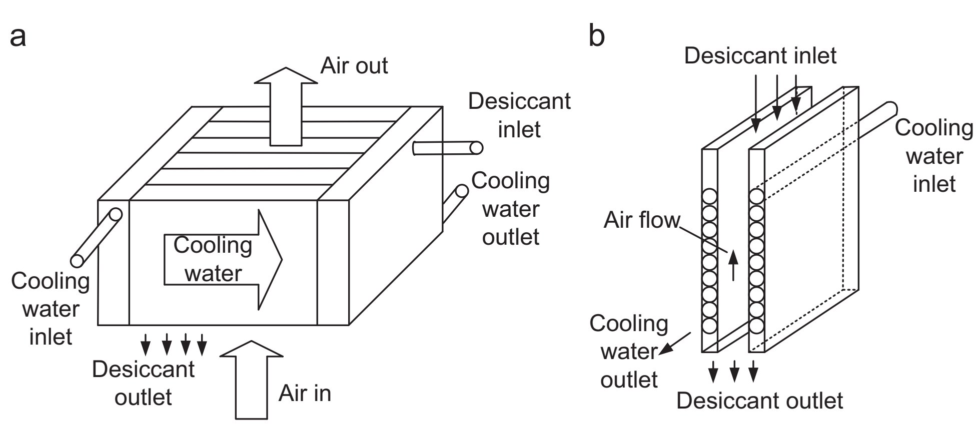


Fig. 4. Schematics of the internally cooled dehumidifier [27]. (a) Sold view; (b) inner view.

evaporator coil bundle over which a lithium chloride–water solution was being sprayed uniformly. The air and the refrigerant were in an overall counter flow configuration. Outside air was brought in direct contact with the desiccant solution on the coil surface for cooling and dehumidification. The weak desiccant solution was collected in a sump underneath the tube bundle. It was then sent to the regenerator. Profiles of humidity and temperature of the process air, the concentration and temperature of the desiccant solution, as well as the quality of refrigerant in the cooling coil were obtained and analyzed in this study.

There was another type of internally cooled dehumidifier, as depicted in Fig. 4. Cooling coils were used to replace the packing material as the air–desiccant contacting surface for heat and mass transfer. Finned tubes were usually employed in this type of dehumidifier to enlarge the air–desiccant contacting areas. Vertical and horizontal distances between the tubes were considered for optimum heat and mass transfer.

Saman and Alizadeh [26] presented another type of dehumidifier, as shown in Fig. 5. As seen, this equipment was a derivative of the internally cooled dehumidifier. It could be described as a direct contact, cross-flow, heat and mass exchanger with a number of flow channels separated from each other by thin plastic plates. The primary air stream was brought into direct contact with desiccant solution spray, while the secondary air stream was brought into contact with water spray in another flow in cross-flow. This dehumidifier made full use of the principles of direct evaporative cooling in one channel to cool the solution film flowing in another channel.

Liu et al. [27] and Yin et al. [28] experimentally and numerically investigated the liquid desiccant air dehumidification with internally cooled dehumidifiers shown in Fig. 4. For such dehumidifiers, the desiccant solution directly contacted the humid air in the dehumidifier. The heat and mass transfer processes occurred between the desiccant solution and the air. The desiccant solution was cooled by indirectly contacting cooling mediums such as water, air, and refrigerant etc. It was found that the internally cooled dehumidifiers provided better dehumidification performances compared to the adiabatic ones. Therefore the internally cooled dehumidifiers provided promising alternatives to liquid desiccant air dehumidification.

These packed columns were efficient. However all of them still had the problem of liquid droplets cross over. So membrane modules were required.

3.2. Membrane modules for liquid desiccant air dehumidification

As mentioned, to prevent desiccant solution droplets from cross-over, semi-permeable membranes could be used to realize air dehumidification. This was the so called membrane-based liquid desiccant air dehumidification technology, as shown in Fig. 1. The selective permeable membranes could be made into parallel-plates or hollow fibers. The air flowed on one side and the solution flowed on the other side of membranes. Heat and moisture were exchanged through the membrane effectively. Other harmful gases or liquid solution were prevented from permeating through the membranes. The parallel-plates or hollow fiber membranes were packed in plastic shells to form parallel-plates membrane modules or hollow fiber membrane modules, respectively. Both the parallel-plates and the hollow fiber membrane types had their own advantages and disadvantages. The former ones were simpler and easier to construct. The pressure losses in the channels were relatively less. The latter ones were more complex and difficult to construct, especially the two ends sealing problems. The pressure losses in the channels were higher. However, the packing densities of the hollow fiber membrane modules were larger and the effectiveness was higher.

The fundamental transport data in the membrane modules were necessary for component design and system optimum. Therefore in recent years the focus of the investigations was on the fluid flow and conjugate heat and mass transfer in these modules.

3.2.1. Parallel-plates membrane module

A parallel-plates membrane module was shown in Fig. 6. It was formed by the membranes stacked together. Equal spacings were kept between neighboring membranes to form flow channels. The solution stream and the air stream flowed alternatively through the parallel channels, in a cross-flow arrangement, for easiness of duct sealing. Other structures were not easy for sealing the liquid fluids [1,2]. The process air was dehumidified by the liquid desiccant, while absorbing moisture from air through the membranes.

The parallel-plates membrane modules had been used as air-to-air heat and mass exchangers before [29,30]. Similarly, due to

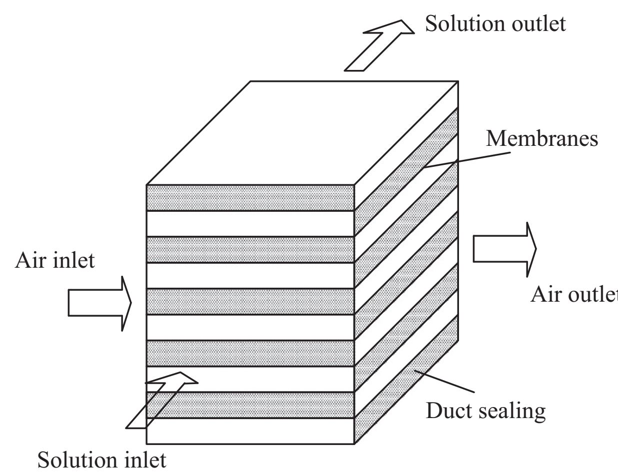


Fig. 6. Structure of a parallel-plate membrane module [37].

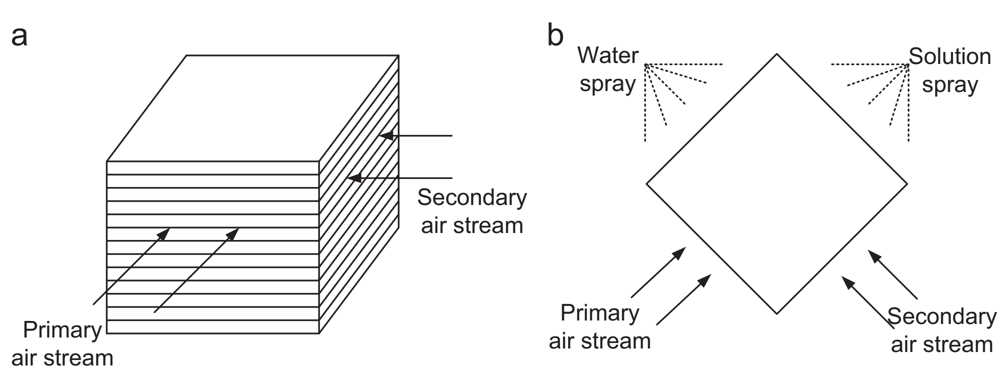


Fig. 5. Cross flow internally cooled dehumidifier [26]. (a) Schematic diagram of air flow directions and (b) fluid sprays contacting with different air streams.

the simple structure and easy fabrication of the parallel-plates membranes, this module was employed in liquid desiccant air dehumidification [31–37]. Mahmud et al. [31] proposed a run-around membrane energy exchanger (RAMEE) system including two quasi-counter flow membrane energy exchangers. Inside each exchanger, a micro-porous membrane separated the air and desiccant solution streams. This membrane only allowed heat and water vapor exchange between the two streams. It was found that the total system effectiveness increased with increasing desiccant flow rate, but decreased as the air flow rate increased. Vail et al. [32] developed a steady-state model to study the heat transfer in a RAMEE system with two quasi-counter flow parallel-plate membrane modules. It was found that the effectiveness of the run-around heat exchanger falls between the effectiveness of similar run-around systems with either two cross-flow exchangers or two counter-flow exchangers. Larson et al. [33] studied the elastic and moisture transfer properties of membrane materials when designing air-to-liquid energy exchangers composed of a series of pressurized membrane channels. The effects of membrane orientation, strain rate and relative humidity on the elastic properties and the effect of humidity on the water vapor resistance were analyzed. Seyed-Ahmadi et al. [34,35] numerically and experimentally studied the coupled heat and moisture transfer in a run-round heat and moisture exchanger with a liquid desiccant. In their study [34], a two dimensional transient model for the coupled heat and moisture transfer in the membrane exchanger was developed. For the simultaneous heat and moisture transfer in the RAMEE, a comparison between numerically modeling results and experimental measurements obtained from laboratory testing for both sensible and latent effectiveness showed satisfactory agreement at different operating conditions. In a separate study [35], the transient behavior of the RAMEE system under different initial and operating conditions was investigated. Li and Ito [36] developed a liquid membrane system containing a surface-soaked liquid membrane with triethylene glycol (TEG) on the hydrophilic-treated surface of the hydrophobic membrane for air dehumidification. A flat-type liquid membrane module with a dual membrane surface is designed. The membrane system recovered water vapor at 4.1 g/h from 70%RH indoor air at 298 K. A simple numerical model based on the permeability of the water vapor was established and experimentally validated.

The above researches [31–36] on the parallel-plate membrane modules used for liquid desiccant air dehumidification were mainly focused on feasibility and energy analysis. The fundamental data such as Nusselt and Sherwood numbers were simply borrowed from some well-known books [38,39]. However, these data were obtained under uniform temperature boundary condition or uniform heat flux boundary condition. They were unable to accurately reflect the real heat and mass transfer properties in the membrane modules for liquid desiccant air dehumidification. It was because that the membrane surface boundary conditions were neither uniform temperature (concentration) or uniform heat flux (mass flux) boundary conditions [29,30]. Rather, they were naturally formed by the coupling between the liquid desiccant and the air stream. It was a conjugate problem.

In order to disclose the features of the conjugate heat and mass transfer in the membrane liquid desiccant air dehumidification, a mathematical model for the cross-flow parallel-plate membrane module, as shown in Fig. 6, was established in [37]. The air and the solution flows were considered to be hydrodynamically fully developed while developing both thermally and in concentration. The governing equations of momentum, heat and mass transfer for the air and the solution streams were set up and solved and experimentally validated.

The calculated fundamental data of Nusselt and Sherwood numbers under various aspect ratios (b/a) were listed in Table 1. It was found that the air side Nusselt number under the conjugate heat and mass transfer condition ($Nu_{C,a}$) was between that under uniform temperature condition (Nu_T) and under heat flux condition (Nu_H). The solution side Nusselt number under the conjugate heat and mass transfer condition ($Nu_{C,s}$) was approximately 15% higher than that in the air side ($Nu_{C,a}$).

3.2.2. Hollow fiber membrane module

3.2.2.1. Parallel flow. As mentioned, the parallel-plate membrane module was simple in structure and easy to be fabricated. The packing density of the module was about 500 m^2/m^3, which was not large enough. However the hollow fiber membrane module, as shown in Fig. 7(a), was more attractive because its packing density was higher and the heat and mass transfer capability was larger. As seen, the concept was similar to a parallel flow tube-and-shell heat exchanger where the two separate fluids flow on the respective sides of the membrane. For air–liquid contacting hollow fiber membrane contactor, the air stream flowed either outside (shell side) or inside (tube side) the tubes. However, in most engineering applications, the solution flowed in the tube side, while the air flowed in the shell side in a counter flow arrangement. The benefit of this flowing configuration was that the pressure drop for the air flow in the shell side was less and the performance was better [40]. The mathematical models of the fluid flow and mass transfer in the gas–liquid hollow fiber membrane contactor were established in several references [41–43].

3.2.2.1.1. Heat and mass transfer through membranes. In gas–liquid membrane contactors, heat and mass were exchanged

Table 1
Fully developed Nusselt and Sherwood numbers in the parallel-plate membrane channels for various aspect ratios [37].

Aspect ratios (b/a) ↓ References →	Nu_H [38,39]	Nu_T [38,39]	Nu_C [29]	Sh_C [29]	$Nu_{C,a}$ [37]	$Sh_{C,a}$ [37]	$Nu_{C,s}$ [37]
1.0	3.61	2.98	1.88	1.89	3.12	3.30	3.41
1.43	3.73	3.08	2.49	2.52	3.23	3.41	3.64
2.0	4.12	3.39	3.06	3.10	3.48	3.65	4.05
3.0	4.79	3.96	4.06	4.00	4.15	4.28	4.74
4.0	5.33	4.44	4.64	4.52	4.61	5.11	5.35
8.0	6.49	5.60	6.06	6.03	5.79	5.83	6.41
50.0	–	–	7.78	7.81	7.54	7.74	7.91
100.0	–	–	8.07	8.05	7.70	7.98	8.08
∞	8.23	7.54	–	–	–	–	–

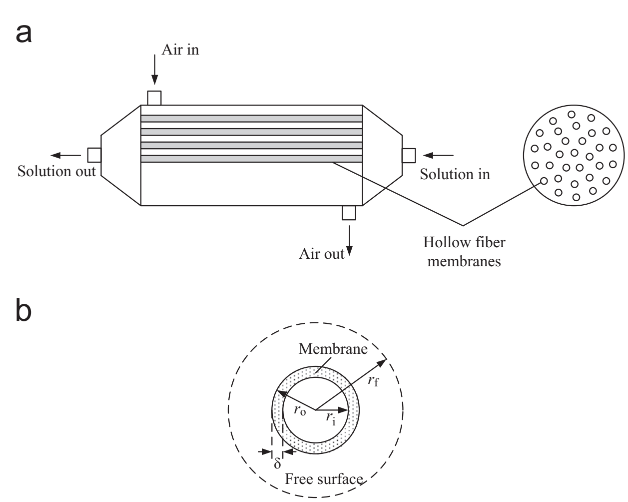


Fig. 7. Schematic of the hollow fiber membrane module and the cell with a free surface model [62]. (a) The shell and the tube structure; (b) the cell with a free surface.

through the membranes between the gas and the solution streams. Heat and mass transfer inside the membranes were assumed isotropic. The membrane was asymmetric in nature. However, it was asymmetric in thickness direction, not on face. Due to the rather small membrane thickness, a resistance in thickness was used, which represented the resistance through the whole membrane. It was like a lumped parameter in thickness. On the directions perpendicular to thickness, it was considered isotropic [30].

As mentioned, both hydrophobic microporous4 and nonporous membranes were commonly used. For the microporous membranes, the effective heat conductivity in the membranes could be obtained by the weighted average of the gas and the solid material [44]. The established theory of gas diffusion in porous media included three mechanisms: Poiseuille flow, Knudsen flow, and/or a combination of them [45]. Viscous Poiseuille flow was bulk, which was non-separating flow caused by total pressure gradients. In the Knudsen regime, the transport was controlled by molecule–wall collision, so that the molecules traveled independently from each other. In contrary, molecule–molecule collisions determined the molecular (ordinary) diffusion. For common gas–liquid membrane contactors, due to the balanced flow, there was no trans-membrane total pressure difference, so there was no bulk viscous Poiseuille flow. The mechanism for gas diffusion was combined Knudsen and ordinary diffusion [44].

For the nonporous membranes, due to the potential virtue of overcoming the crossover problem encountered in the traditional packed beds liquid desiccant air dehumidification technology, they were more attractive and more commonly employed. The nonporous membranes were usually modified by coating with a dense silicone or gel layer. Therefore the membranes were highly hydrophobic. Knudsen diffusion was the predominant mechanism of water vapor transporting through the membrane. So the resistance in membrane itself was considered as a lumped parameter, as described in [37].

3.2.2.1.2. Fluid flow and mass transfer in tube side. Due to the rather small diameter of fiber tubes (in the order of 1.5 mm), the solution flow was in the laminar region (< 2300). A set of differential equations was obtained from mass balance inside the fibers. The solution could be derived using the method suggested by Leveque and Graetz [46,47]. The local values of Sherwood numbers were calculated in terms of Graetz solution and the average Sherwood numbers were obtained as series equations. The equations for the local Sherwood numbers converged rapidly for small values of Graetz number ($Gz = ud_i^2/DL$) [47]. Under these asymptotic conditions, the average Sherwood number could be calculated by

$$Sh = \frac{k_s d_i}{D}, \quad Gz < 10 \tag{1}$$

Another asymptotic solution was obtained by the Leveque equation [46] by assuming that the concentration boundary layer was restricted to a thin region near the wall of the fiber tubes. This approximation was valid in cases of high velocities through relatively short fibers in laminar flow. One important consequence of this assumption was that the Leveque solution was suitable when Gz numbers were greater than 20. The Leveque solution was given by

$$Sh = 1.62(Gz)^{1/3}, \quad Gz > 20 \tag{2}$$

The Graetz–Levegue solution was employed to predict the fiber side mass transfer coefficient. Kreulen et al. [48] gave the generalized solution of Graetz–Levegue equation by curve fitting of Eqs. (1) and (2), which was also valid for the transition region not covered by Eqs. (1) and (2):

$$Sh = (3.67^3 + 1.62^2 Gz)^{1/3}, \quad 10 < Gz < 20 \tag{3}$$

3.2.2.1.3. Fluid flow and mass transfer in the shell side. One of the most commonly used parallel flow hollow fiber module geometries was the shell and tube configuration with a bundle of fiber tubes, populated axially in the cross-section. The fluid flow and heat mass transfer problems outside the hollow fiber tubes were more complex than those in the inner tubes. The performances of the fluid flow and heat mass transfer in the shell side in these modules varied significantly, which were caused by a number of factors including the irregularity of fiber spacing within the module, polydispersity of fiber diameters, movement during operation of fibers, influence of the wall of the module, and inlet and outlet effects. Happel's free surface model [49] was an approach available to model the fluid flow and heat mass transfer in the shell side to reflect the fiber-to-fiber interactions. The difficulty of a direct modeling of the whole bundle on a fiber-to-fiber basis could be overcome by the free surface model. According to this model, it was considered that each fiber in the shell space was surrounded by a fluid envelope, and there was no momentum, heat or mass transfer on the outer free surface. The fibers were assumed to be distributed homogeneously and the flow was purely axial. The bundle was comprised of a series of such free surface cells. Each cell had only one fiber in the center and was surrounded by homogeneous fluid [49]. The cross section of the tube channel was a circle, while the cross section of the shell side channel was an annulus, as depicted in Fig. 7(b). The mass conservation equation for the fluid flow outside fibers was similar to that in the inner tubes. It was suggested that the Happel's free surface model to be used to characterize the out fibers velocity profile [49]. Although the fluid flow outside the fiber tubes was not absolutely according with the results obtained based on the free surface model, it had been extensively used for the parallel flow hollow fiber membrane contactor [50].

For the free surface model, the fibers were considered to be populated homogeneously in the shell side. A number of studies had been carried out on the theoretical background of the fluid flow and heat mass transfer in the case of uniform distribution of solid cylinders and hollow fiber arrays [51,52]. However, the fibers can be packed uniformly or randomly. Further, it had been long recognized that uniform fiber distribution was an unrealistic assumption for most hollow fiber modules, and the fluid flow through the maldistributed hollow fibers was often encountered in shell-side flow [53,54]. Recently, Zhang [55] proposed a fractal model approach to investigate the heat and mass transfer in a randomly packed counter flow hollow fiber membrane module. The disordered nature of hollow fiber distributions in the module exhibited the existence of a fractal structure formed by the voids between the fibers. Based on the fractal theory developed, the shell side flow distribution and convective heat and mass transfer were investigated and experimentally validated. The results showed that the higher the packing density was, the less the fractal dimension was, and the less the non-uniformity of the flow distribution was. Correlations were proposed for the estimation of friction factor and Sherwood numbers considering the degree of irregularity.

Shell side mass transfer coefficients of the parallel flow hollow fiber membrane modules were useful for module design. The mass transfer coefficients were commonly described in the form of $Sh = f(\varphi, Re, Sc)$. Where φ was packing fraction; Re and Sc were Reynolds and Schmidt number, respectively. Shell side mass transfer correlations for the parallel flow hollow fiber membrane modules had been determined in a number of studies [53–61], which are listed in Table 2.

3.2.2.1.4. Conjugate heat and mass transfer inside and outside the fiber tubes. The above-mentioned references [41–61] were focused on the fluid flow and heat and mass transfer in the fiber tubes or

Table 2
Shell side mass transfer correlations for parallel flow hollow fiber membrane modules.

Correlations	Conditions	References
$Sh=(0.53-0.58\varphi)Re^{0.53}Sc^{0.33}$	$21<Re<324$; $0.32<\varphi<0.76$	[53]
$Sh=5.85(1-\varphi)(D_h/L)Re^{0.6}Sc^{0.33}$	$0<Re<500$; $0.04<\varphi<0.4$	[54]
$Sh=(14.06\varphi^4-29.21\varphi^3+22.59\varphi^2-7.71\varphi+1.03)Re^{0.33}Sc^{0.33}\psi$ where, $\psi=0.882D_f-0.535$	Laminar, $1.6<D_f<1.9$	[55]
$Sh=1.25(ReD_h/L)^{0.93}Sc^{0.33}$	$Re<500$; $\varphi=0.03$	[56]
$Sh=1.38Re^{0.34}Sc^{0.33}$	$32<Re<25$; $\varphi=0.7$	[56]
$Sh=0.90Re^{0.40}Sc^{0.33}$	$32<Re<25$; $\varphi=0.07$	[56]
$Sh=(0.304\varphi^2-0.3421\varphi+0.0015)Re^{0.9}Sc^{0.33}$	$32<Re<1287$; $0.1<\varphi<0.7$	[57]
$Sh=0.61Re^{0.363}Sc^{0.33}$	$0.6<Re<49$; $\varphi=0.003$	[58]
$Sh=(0.163+0.27\varphi)\left(\frac{u}{D_hL}\right)^{0.6}$	$178<Re<1194$	[59]
$Sh=0.41\left(\frac{1}{n_f}\right)\left(\frac{D_o}{d_o}\right)^2\left(\frac{D_h}{L}\right)^2Re^{0.33}Sc^{0.33}$	$10<Re<300$; $0.0506<\varphi<0.157$	[60]
$Sh=(Sh_1^3+Sh_2^3+Sh_3^3)^{1/3}$ where, $Sh_1=3.66+1.2(\sqrt{\varphi})^{-0.8}$; $Sh_2=1.615(1+0.14(\sqrt{\varphi})^{-0.5})^3\left(\frac{Re\,Sc\,D_h}{L}\right)^{0.5}$; $Sh_3=\left(\frac{2}{1+22Sc}\right)^{1/6}\left(\frac{Re\,Sc\,D_h}{L}\right)^{0.5}$	Laminar, $0.10<\varphi<0.75$	[61]

Table 3
Fully developed (fRe), Nusselt and Sherwood numbers for the annular channel in the counter flow hollow fiber membrane module [62].

Packing fraction (φ)	r_o/r_f	Nu_T	Nu_H	$Nu_{C,a}$	$Sh_{C,a}$	(fRe)
0.063	0.25	7.05	7.49	7.44	7.30	13.81
0.162	0.40	5.51	5.97	5.94	5.84	16.72
0.203	0.45	5.24	5.67	5.64	5.57	17.53
0.253	0.50	4.99	5.43	5.40	5.34	18.39
0.281	0.53	4.89	5.32	5.30	5.22	18.81
0.360	0.60	4.66	5.10	5.07	4.98	19.85
0.422	0.65	4.52	4.95	4.92	4.86	20.55
0.491	0.70	4.41	4.81	4.80	4.75	21.25
0.563	0.75	4.31	4.72	4.71	4.64	21.91
0.641	0.80	4.24	4.63	4.60	4.55	22.56
0.689	0.83	4.20	4.59	4.56	4.50	22.92

outside the tubes. However the conjugate heat and mass transfer inside and outside the fibers were not seriously taken into account before.

The parallel flow hollow fiber membrane module was similar to a parallel flow tube-and-shell heat exchanger. The fluid flow and heat mass transfer in the parallel flow heat exchanger were studied in several researches [38,39]. The heat and mass transfer coefficients in the inner tube side and the shell side in the module were simply borrowed from well-established Nusselt and Sherwood correlations for traditional parallel flow tube-and-shell heat exchangers. However, these correlations were not suitable for the membrane-based liquid desiccant air dehumidification process because the membrane surfaces boundary conditions were different. Moreover, the air and the solution streams were conjugated together through the membranes. The wall boundary conditions were neither uniform temperature nor uniform heat flux boundary conditions. It was a conjugate problem.

In order to obtain the more accurate heat and mass transfer coefficients in the counter flow hollow fiber membrane module used for liquid desiccant air dehumidification, Zhang et al. [62] investigated the conjugate heat and mass transfer in a counter flow hollow fiber membrane module for liquid desiccant air dehumidification based on the free surface model. A representative cell comprising of a single fiber, the liquid desiccant flowing inside the fiber and the air stream flowing outside the fiber, as shown in Fig. 7(b), was considered. The equations governing the fluid flow and heat and mass transfer in the two streams were solved together with the corresponding boundary conditions. The local and mean Nusselt and Sherwood numbers under the conjugate heat and mass transfer boundary conditions were then obtained and experimentally validated. It was found that the solution side local Nusselt number ($Nu_{C,s}$) was nearly equal to Nu_H. For the air flow, the fully developed (fRe), Nusselt and Sherwood numbers were summarized in Table 3. As seen, the fully developed Nusselt numbers for air stream $Nu_{C,a}$ was between Nu_H and Nu_T. $Nu_{C,a}$ was closer to Nu_H. The Sherwood numbers ($Sh_{C,a}$) were somewhat less than the air side $Nu_{C,a}$. The obtained data provided the fundamentals for the future design of the counter flow hollow fiber membrane module used for liquid desiccant air dehumidification.

3.2.2.2. Cross-flow. Counter flow was the most commonly used arrangement for membrane contactors. However this structure had a potential disadvantage of rather large pressure drop losses. To address this problem, the cross-flow hollow fiber membrane module, as shown in Fig. 8(a), was proposed for liquid desiccant air dehumidification [63–71]. The concept was similar to a cross-flow tube-and-shell heat exchanger. The solution stream flowed in tube side, while the air stream flowed across the fiber bank in the shell side in a cross-flow arrangement. Bergero and Chiari [63] experimentally and theoretically investigated the air dehumidification process carried out in a cross-flow hollow fiber membrane contactor. Air flow rates ranging from 30 to 80 m^3/h were considered. Experimental results showed that the heat and mass transfer efficiencies were high. Kneifel et al. [64] studied the coated polyetherimide hollow fiber membranes with respect to the water vapor permeance. The measurements were carried out under common operating conditions using prototype modules and LiCl as the liquid desiccant. Influences of both the support membranes and the coating layer were determined. It was shown that the negative effect of the coating layer on the permeance could be restricted to a permeance loss of about 20% by applying a very thin coating layer. Johnson et al. [65] described the potential use of hollow fiber membranes in evaporative cooling applications for space air-conditioning. Duct-mountable hollow fiber membrane bundles were used as contactors for the delivery of liquid water to an air stream in a heating, ventilating air-conditioning duct. A series of experimental and analytical parametric studies were performed to investigate the heat and mass transfer phenomena in evaporative

cooling with hollow fiber membranes. Dijkink et al. [66] experimentally studied humidity control using a hollow fiber membrane contactor which allowed adequate transfer of water vapor between the air and a liquid desiccant. The membrane was made of polyetherimide (PEI), coated on the inside with a thin non-porous silicone layer. The desiccant was a dilute aqueous glycerol solution. Isetti et al. [67] proposed a new approach to absorption air-handling systems working with liquid desiccants. Theoretical analysis was conducted to study the influence of different affecting vapor mass flux through a hydrophobic membrane. It was found that considerable vapor flux could be exchanged to/from a liquid desiccant and an air stream through the membrane, suggesting the feasibility of using compact membrane absorber and desorber units in air handling.

The fluid flow and heat mass transfer in the inner tubes were actually similar to those in the common metal-formed round channels. The fluid flow and heat and mass transfer in the shell side were more complex than those in the inner tubes. In order to solve the fluid flow and heat transfer problems in tube-and-shell heat exchangers, two distinct approaches were available to describe the fiber-to-fiber interactions: free surface model and periodic unit cell model.

3.2.2.2.1. Free surface model. In the first scheme, modeling of the fiber-to-fiber interactions was relied on the use of the so-called free surface model [49]. In this approach, the viscous interactions between the fluid and the fiber bank were mimicked by enclosing each fiber into a hypothetical concentric fiber envelope of the fluid, as depicted in Fig. 8(b). The packing fraction of each unit cell was equal to the overall mean packing fraction of the whole fiber bank. The free surface model had gained wide acceptance in predicting macroscopic transport phenomena in the fluid flow and heat transfer across the cylinder bundle. It had been found that the fluid flow of Newton and non-Newton and heat transfer across the tube bank could be well predicted by the free surface model. The pressure drag coefficient, friction drag coefficient, and Nusselt number and their various tendencies were obtained and analyzed [72–77]. In engineering applications, the Nusselt numbers for the fluid flow and heat transfer across the tube bank were the necessities for the module design. Therefore the correlations for the average Nusselt numbers based on the free surface model are summarized in Table 4.

These data in Table 4 were obtained under uniform temperature or uniform heat flux boundary conditions. They were not suitable for the membrane module for liquid desiccant air dehumidification because the membrane surfaces boundary conditions were neither uniform temperature (concentration) nor uniform heat flux (mass flux) boundary conditions [38,39]. Rather, they were naturally formed by the coupling between the liquid desiccant and the air stream. It was a conjugate problem. At last, the heat and mass transfer were strongly coupled because of vapor condensation on the membrane surfaces.

The cross-flow hollow fiber membrane contactor, as shown in Fig. 8(a), was used for liquid desiccant air dehumidification. The solution stream flowed inside the fiber tubes, while the air stream flowed across a bundle of fibers in the shell side. A direct modeling of the whole bundle on a fiber-to-fiber basis was difficult to perform since the fibers were numerous, usually 2000–12,000 in a contactor $20\times20\ \mathrm{cm}^2$ in cross section. To solve this problem, Happel's free surface model was used to model the fluid flow and heat and mass transfer in the module for liquid desiccant air dehumidification [68,69].

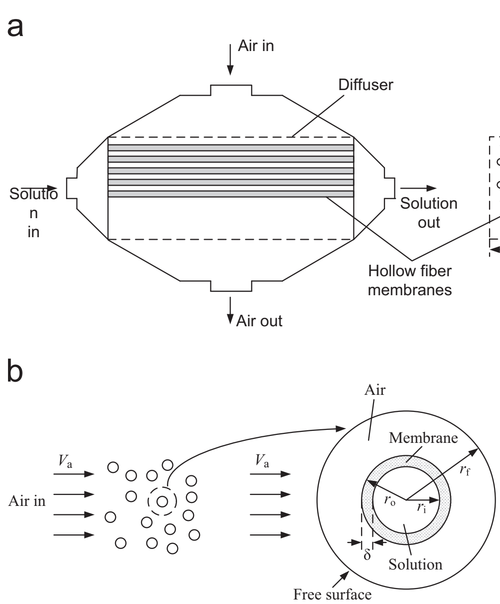


Fig. 8. Schematic of a cross flow hollow fiber membrane contactor, a free surface cell selected as the calculation domain [68,69]. (a) The shell and the tube structure; (b) the free surface cell.

Table 4
Correlations of average Nusselt numbers for fluid flow across tube bank.

Correlations	Conditions	References
$Nu=0.082Re^{0.5}+0.734Re^{x}$ where $x=0.05+0.226Re^{0.085}$	Air flow, free surface model, $Re\le200$	[77]
$Nu=0.8Re^{0.4}Pr^{0.37}$	In-line arrays, free surface model, φ=0.2, Re=40, 120, 400 and 800, Pr=0.1, 1 and 10	[78]
$Nu=0.78Re^{0.45}Pr^{0.38}$	Staggered arrays, free surface model, φ=0.2, Re=40, 120, 400 and 800, Pr=0.1, 1 and 10	[78]
$Nu=CRe^{n}$, $Nu\|_{N<10}=C_1Nu\|_{N\ge10}$	Air flow, in-line or staggered arrangements, $N<10$, C, C_1n are given in [38,39]	[38,39]
$Nu=0.271Re^{0.583}$	The first row	[82]
$Nu=0.511Re^{0.57}$	The third row	[82]
$Nu=0.33Re^{0.6}Pr^{1/3}$	Staggered arrangement, N (tube rows) > 10, 10 < Re < 40000	[86]
$Nu=C\ Re^{n}$	Air flow, in-line or staggered arrangements, $N>10$, C is given in [87–89]	[87–89]
$Nu=0.32F_aRe^{0.61}Pr^{0.31}$	Air flow, in-line or staggered arrangements, $N>10$, F_a can be referenced form [89]	[89]
$Nu=F_aCRe^{n}Pr^{m}$	$N\ge16$ F_a, C, m and n are given in [38,39]	[90]
$Nu=0.34F_aRe^{0.61}Pr^{0.31}$ where $F_a=1+(a+7.17/a-6.52)[0.266/(b-0.8)^2-0.12]\sqrt{1000/Re}$	Air flow, in-line arrangement, $N>10$	[91]
$Nu=0.35F_aRe^{0.57}Pr^{0.31}$ where $F_a=1+0.1a+0.34/b$	Air flow, staggered arrangement, $N>10$	[91]

Table 5
The total drag coefficient and the overall mean Nusselt and Sherwood numbers for the air flow across a single fiber with a free surface, Re_a=50–600 [68,69].

φ↓	r_o/r_f↓	$Nu_{ave,T}$↓	$Nu_{ave,H}$↓	$Nu_{ave,a}$↓	$Sh_{ave,a}$↓	C_D↓	$Nu_{ave,T}$↓	$Nu_{ave,H}$↓	$Nu_{ave,a}$↓	$Sh_{ave,a}$↓	C_D↓
		$Re_a=50$					$Re_a=100$				
0.160	0.40	4.65	5.39	5.54	5.72	4.03	6.23	7.18	7.11	7.36	3.25
0.200	0.45	4.87	5.58	5.90	6.13	4.81	6.51	7.51	7.49	7.82	3.85
0.265	0.51	5.25	6.01	6.51	6.85	6.35	6.98	8.05	8.15	8.59	5.01
0.362	0.60	5.91	6.74	7.58	8.13	9.86	7.79	8.99	9.26	10.00	7.59
0.490	0.70	7.14	8.05	9.41	10.49	19.09	9.19	10.58	11.10	12.54	14.21
0.562	0.75	8.21	9.12	10.76	12.42	29.72	10.26	11.77	12.41	14.58	21.52
0.642	0.80	10.01	10.89	12.71	15.57	54.33	11.93	13.57	14.21	17.70	37.23
		$Re_a=200$					$Re_a=250$				
0.160	0.40	8.57	9.88	9.61	9.87	2.80	9.72	11.21	10.66	10.96	2.73
0.200	0.45	8.93	10.28	10.01	10.37	3.29	10.06	11.62	11.08	11.48	3.21
0.265	0.51	9.47	10.95	11.01	11.49	4.24	10.64	12.32	11.78	12.36	4.12
0.362	0.60	10.45	12.12	12.39	12.71	6.29	11.67	13.55	12.96	13.97	6.09
0.490	0.70	12.20	14.16	14.82	15.53	11.35	13.52	15.72	14.93	16.82	10.92
0.562	0.75	13.52	15.69	16.58	17.77	16.84	14.95	17.37	16.36	19.11	16.07
0.642	0.80	15.48	17.92	19.20	21.27	28.37	17.07	19.81	20.32	22.65	26.82
		$Re_a=300$					$Re_a=400$				
0.160	0.40	10.78	12.35	11.91	11.99	2.72	12.53	14.31	13.79	13.83	2.61
0.200	0.45	11.13	12.81	12.44	12.53	3.20	12.91	14.81	14.36	14.42	3.07
0.265	0.51	11.73	13.54	13.31	13.43	4.08	13.56	15.63	15.32	15.38	3.92
0.362	0.60	12.83	14.86	14.92	15.05	5.93	14.74	17.07	17.04	17.10	5.68
0.490	0.70	14.79	17.17	17.87	17.93	10.15	16.88	19.61	20.21	20.19	9.73
0.562	0.75	16.32	18.92	20.23	20.21	14.26	18.53	21.54	22.71	22.56	13.67
0.642	0.80	18.68	21.58	23.94	23.83	22.32	21.06	24.41	26.61	26.24	20.91
		$Re_a=500$					$Re_a=600$				
0.160	0.40	14.09	16.06	15.49	15.46	2.54	15.52	17.64	17.05	16.94	2.48
0.200	0.45	14.52	16.61	16.12	16.10	2.98	15.98	18.25	17.72	17.64	2.92
0.265	0.51	15.21	17.51	17.15	17.14	3.81	16.70	19.22	18.84	18.74	3.73
0.362	0.60	16.47	19.05	18.98	18.95	5.51	18.07	20.89	20.79	20.65	5.40
0.490	0.70	18.76	21.80	22.36	22.21	9.45	20.49	23.81	24.34	24.07	9.24
0.562	0.75	20.54	23.89	25.03	24.74	13.33	22.40	26.07	27.16	26.74	13.07
0.642	0.80	23.22	26.97	29.10	28.53	20.40	25.25	29.37	31.47	30.74	20.17

Zhang et al. [68] investigated the laminar fluid flow and heat mass transfer in the cross-flow hollow fiber membrane contactor for liquid desiccant air dehumidification. The total drag coefficient, Nusselt and Sherwood numbers under naturally formed boundary condition were obtained for the air flow Reynolds number (Re_a) ranging from 50 to 300.

For the same membrane contactor, Huang et al. [69] noted that the laminar model established in [68] was not suitable when Re_a was larger than 300. Therefore a low-Re $k-\varepsilon$ turbulence model [69] was employed to describe the turbulent fluid flow and heat mass transfer across the fiber bundle in the membrane contactor. The momentum, energy and mass governing equations for the air and the solution flows were solved and experimentally validated. The total drag coefficient, Nusselt and Sherwood numbers under the naturally formed boundary conditions were obtained for Re_a=300–600. Both for the laminar model (Re_a=50–300) and the turbulent model (Re_a=300–600), the solution side $Nu_{C,s}$ was almost equal to Nu_H (=4.36), but larger than Nu_T (=3.66) [38,39]. The total drag coefficient, the overall mean Nusselt and Sherwood numbers for the air flow in the shell side are listed in Table 5. As seen, air side $Nu_{ave,a}$ was between $Nu_{ave,T}$ and $Nu_{ave,H}$ for sparsely distributed contactors (low φ), but $Nu_{ave,a}$ was larger than $Nu_{ave,H}$ for densely populated contactors (high φ). These values were useful for future design of the cross-flow hollow fiber membrane module used for liquid desiccant air dehumidification.

3.2.2.2.2. Periodic unit cell model. For the second approach, the momentum and energy conservation equations were solved analytically and/or numerically for periodic arrays with different geometrical arrangements. For instance, Wung and Chen [78,79] investigated the fluid flow and heat transfer over the circular cylinder banks with in-line and staggered arrangements. The Navier–Stokes and the energy equations were solved under the Reynolds numbers of 40, 120, 400 and 800 and under the Prandtl numbers of 0.1, 1.0 and 10.0. Martin et al. [80] numerically studied the convective heat transfer in sparse periodic (square and triangular) arrays of cylinders in cross-flow (packing fraction, $\varphi<0.2$). Effects of the thermal boundary conditions, i.e., a uniform temperature or uniform heat flux imposed on the cylinder surfaces were investigated. Wilson and Bassiouny [81] numerically studied the heat transfer between the air and in-line as well as staggered arrays comprising two rows of cylinders in fully turbulent region. A standard $k-\varepsilon$ turbulent model was employed and uniform temperature condition was imposed on the surface of the cylinders. Yoo et al. [82] reported the local heat transfer coefficients for various tube spacings, tube locations and Reynolds numbers. Correlations for the average heat transfer coefficients were developed and compared with the conventional ones. Kim et al. [83] experimentally investigated the effects of scale roughness, cylinder spacing and Reynolds number on the heat transfer in the staggered tube banks. Buyruk [84] predicted the heat transfer characteristics in tube banks with tube arrangement and flow condition at low Reynolds numbers below 400. Lange et al. [85] presented a summary of results of numerical investigations of the two-dimensional flow around a heated circular cylinder located in a laminar cross-flow. Numerical investigations were carried out for the Reynolds number range $10^{-4}<Re<200$ and for temperature loadings of 1.003–1.5. The temperature dependence of the fluid properties (air) had been taken into account. The correlations for the average Nusselt numbers based on the periodic unit cell model [78,86–91] are also summarized in Table 4.

To accumulate the fundamental data in the membrane contactor, Zhang and Huang investigated the friction factor and the Nusselt and Sherwood numbers in a cross flow fiber bundle with a simplified free surface model [68,69]. The results, to some extent,

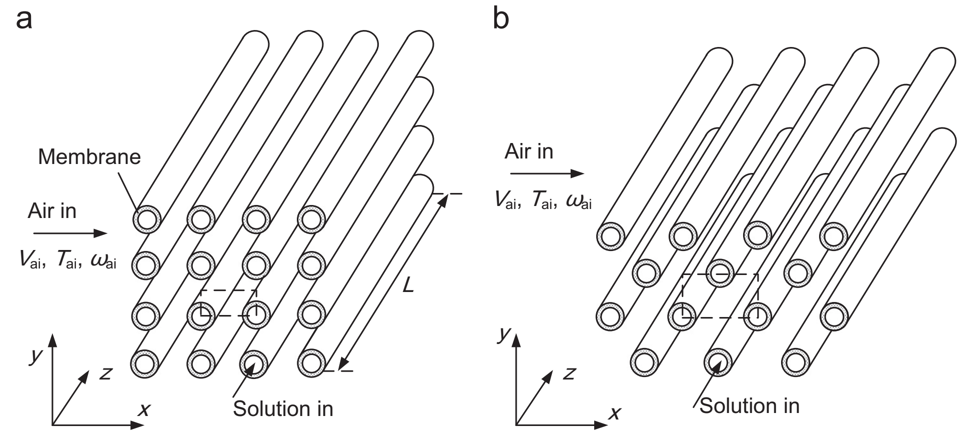


Fig. 9. Schematic of a cross flow hollow fiber membrane bundle [70,71]. (a) In-line; (b) staggered. The area surrounded by the dash line is the representative calculation domain.

Table 6
The friction factor and the mean Nusselt and Sherwood numbers for the air stream across the hollow fiber membrane bundle, with in-line arrangement, $S_T=S_L$, $Re_a=50$–600 [70,71].

$S_L/(2r_o)$↓	φ↓	$Nu_{ave,T}$↓	$Nu_{ave,H}$↓	$Nu_{ave,a}$↓	$Sh_{ave,a}$↓	f_a↓	$Nu_{ave,T}$↓	$Nu_{ave,H}$↓	$Nu_{ave,a}$↓	$Sh_{ave,a}$↓	f_a↓
		$Re_a=50$					$Re_a=100$				
1.25	0.502	7.25	19.56	7.68	18.85	0.880	7.86	20.25	8.46	19.81	0.517
1.5	0.349	4.90	9.11	4.75	8.78	0.554	5.31	9.29	5.99	9.02	0.318
1.75	0.256	3.96	6.07	4.01	5.85	0.411	4.30	6.46	5.09	6.27	0.232
2.0	0.196	3.43	4.71	3.44	4.56	0.327	3.74	5.09	4.56	4.97	0.180
2.25	0.155	3.07	3.92	3.04	3.81	0.270	3.33	4.24	4.07	4.18	0.144
2.5	0.125	2.81	3.39	2.69	3.31	0.229	3.02	3.62	3.59	3.62	0.115
		$Re_a=200$					$Re_a=300$				
1.25	0.502	9.25	21.32	9.44	20.21	0.346	10.74	22.58	10.69	21.26	0.293
1.5	0.349	6.27	9.68	6.62	9.34	0.213	7.36	10.40	7.11	9.88	0.183
1.75	0.256	5.13	6.94	5.82	6.72	0.157	6.13	7.53	6.15	7.23	0.140
2.0	0.196	4.46	5.52	5.52	5.43	0.121	5.41	5.98	5.93	5.88	0.111
2.25	0.155	3.93	4.54	5.24	4.60	0.0899	4.50	4.83	5.78	4.98	0.0828
2.5	0.125	3.31	3.78	4.96	4.02	0.0632	3.58	3.83	5.58	4.29	0.0488
		$Re_a=300$					$Re_a=400$				
1.25	0.502	13.86	19.12	11.75	18.88	0.362	15.23	21.00	15.49	20.21	0.328
1.5	0.349	8.85	10.96	7.92	10.56	0.227	10.07	12.52	8.98	11.72	0.211
1.75	0.256	7.18	8.52	6.84	7.90	0.172	8.34	10.20	7.67	8.89	0.164
2.0	0.196	6.30	7.32	6.51	6.50	0.135	7.45	8.93	7.03	7.36	0.131
2.25	0.155	5.62	6.22	6.30	5.53	0.106	6.76	7.71	6.95	6.27	0.104
2.5	0.125	4.89	5.68	6.03	4.75	0.0884	5.84	6.72	6.62	5.32	0.0875
		$Re_a=500$					$Re_a=600$				
1.25	0.502	16.70	23.06	17.98	21.97	0.310	18.19	25.31	20.66	23.91	0.299
1.5	0.349	11.33	14.44	12.66	12.98	0.203	12.57	16.48	14.93	14.31	0.198
1.75	0.256	9.52	12.03	8.48	9.92	0.160	10.70	13.86	12.28	11.02	0.156
2.0	0.196	8.62	10.60	7.78	8.26	0.129	9.78	12.19	8.59	9.15	0.128
2.25	0.155	7.95	9.24	7.55	7.02	0.103	9.14	10.70	8.30	7.71	0.102
2.5	0.125	6.53	7.82	7.37	5.95	0.0868	8.50	9.91	8.12	6.38	0.0852

were helpful for module design. However, a free surface model was only a coarse approximation, and the interactions between the neighboring fibers could not be considered. To account for these interactions between the neighboring fibers, Zhang and Huang [70,71] took a new approach: the fluid in the fibers was modeled in together with the neighboring fibers. The calculating domains were selected as the periodic area surrounded by the neighboring fibers, as shown in Fig. 9. On these representative cells, both the laminar [70] and the turbulent [71] fluid flow and the conjugate heat mass transfer between the fluids and these surrounding fibers were investigated. The Nusselt and Sherwood numbers accounting for these interactions under naturally formed boundary conditions were obtained for $Re_a=50$–600. The results for the in-line and the staggered arrangements are listed in Tables 6 and 7, respectively. They were compared to those data calculated with the free surface, which were listed in Table 5. It had been found that the free surface model was applicable only when the packing fraction (φ) was less than 0.2. The fundamental data listed were useful for future module design and system optimum.

4. Applications of membrane-based liquid desiccant air dehumidification

A comprehensive liquid desiccant air dehumidification system usually included the components such as dehumidifier, regenerator, pumps, and heat exchangers and so on. To improve the energy utilization ratio, combinations of air dehumidification systems to other air-conditioning systems became a hot topic. Xiao et al. [92] proposed a novel dedicated outdoor air system (DOAS) that adopted lithium chloride solution as liquid desiccant to process

Table 7
The friction factor and the mean Nusselt and Sherwood numbers for the air stream across the hollow fiber membrane bundle, with staggered arrangement, $S_T = S_L$, $Re_a = 50$–600 [70,71].

$S_L/(2r_o)$↓	φ↓	$Nu_{ave,T}$↓	$Nu_{ave,H}$↓	$Nu_{ave,a}$↓	$Sh_{ave,a}$↓	f_a↓	$Nu_{ave,T}$↓	$Nu_{ave,H}$↓	$Nu_{ave,a}$↓	$Sh_{ave,a}$↓	f_a↓
		$Re_a = 50$					$Re_a = 100$				
1.25	0.502	12.84	18.19	12.73	17.62	1.343	16.45	21.37	15.15	20.29	1.004
1.5	0.349	9.72	12.53	6.85	11.88	1.059	12.09	15.23	10.64	14.71	0.786
1.75	0.256	7.93	10.50	5.41	10.04	0.903	9.93	12.66	8.17	12.41	0.670
2.0	0.196	7.01	9.42	4.40	9.14	0.777	8.63	11.37	6.81	11.26	0.577
2.25	0.155	6.41	8.74	3.69	8.60	0.691	7.81	10.59	5.87	10.57	0.515
2.5	0.125	5.91	8.25	3.18	8.21	0.614	7.23	10.05	5.18	10.10	0.456
		$Re_a = 200$					$Re_a = 300$				
1.25	0.502	22.04	27.17	20.16	25.92	0.773	26.46	31.62	26.28	30.26	0.653
1.5	0.349	15.63	18.79	14.38	18.29	0.615	18.61	21.71	18.57	21.10	0.538
1.75	0.256	12.75	15.63	11.51	15.32	0.533	15.28	18.16	14.27	17.69	0.473
2.0	0.196	11.14	14.15	9.79	13.92	0.460	13.46	16.54	12.38	16.12	0.421
2.25	0.155	10.12	13.28	8.28	13.09	0.413	12.31	15.61	11.11	15.24	0.364
2.5	0.125	9.41	12.71	7.31	12.56	0.344	11.55	15.02	10.21	14.67	0.320
		$Re_a = 300$					$Re_a = 400$				
1.25	0.502	26.60	31.86	25.14	30.46	0.690	30.68	35.72	29.46	34.19	0.645
1.5	0.349	18.75	21.88	17.78	21.22	0.518	21.62	24.57	20.88	23.74	0.487
1.75	0.256	15.39	18.33	14.44	17.82	0.431	17.84	21.69	17.12	20.01	0.408
2.0	0.196	13.31	17.62	12.29	17.07	0.362	15.21	20.42	14.53	19.63	0.340
2.25	0.155	12.38	15.82	11.22	15.40	0.317	14.51	18.07	13.57	17.47	0.300
2.5	0.125	11.58	15.23	10.31	14.85	0.276	13.62	17.51	12.56	16.94	0.262
		$Re_a = 500$					$Re_a = 600$				
1.25	0.502	34.58	40.02	33.52	37.52	0.611	38.37	43.92	37.33	40.58	0.592
1.5	0.349	24.39	27.06	23.80	26.06	0.471	27.10	29.40	26.59	28.23	0.460
1.75	0.256	20.22	22.88	19.67	22.03	0.395	22.53	24.94	22.13	23.95	0.386
2.0	0.196	16.91	23.11	16.57	22.10	0.325	18.42	25.65	18.43	24.45	0.313
2.25	0.155	16.55	20.20	15.87	19.43	0.291	18.51	22.26	18.05	21.31	0.284
2.5	0.125	15.55	19.72	14.74	18.86	0.253	17.39	21.85	16.89	20.92	0.247

supply air. The DOAS mainly consisted of a membrane-based total heat exchanger, a dehumidifier, a regenerator and a dry cooling coil. Control strategies for the supply air dehumidification, cooling process, and the desiccant solution regeneration process were developed and verified. The results showed that the DOAS was more suitable for hot and humid climates. The effects of the total heat exchanger on the performance of the DOAS were also evaluated. It could improve the system energy performance by 19.9–34.8%. Nayak et al. [93] presented a combined heat and power system involving on-site or near-site generation of electricity from thermal energy from the power generation processes. This research was carried out in a four-story educational office building. The liquid desiccant unit dehumidified and cooled the ventilation air to the building and supplied it to the mixed air section of the roof top unit. They discussed the various aspects involved in the design and installation of the system such as the heat recovery loop design and the electrical interconnection with the building load bus. Test results were also presented and the performance was compared to a traditional power plant with a conventional heating, ventilating, and air-conditioning system. Sayegh et al. [94] evaluated and compared two air dehumidification methods which were the hybrid systems: refrigeration cycle-rotary desiccant and the heat exchanger cycle. It was found that the coefficient of performance and the cooling effect of the heat exchanger cycle were lower than those of the conventional cooling system. The coefficient of performance and the cooling effect of the hybrid system were close to those of the conventional cooling system. Li and Yang [95] presented the numerical simulation results of an open cycle liquid desiccant dehumidification system. They attempted to obtain the best configurations of the solar assisted air-conditioning system and to validate the feasibility of using a liquid desiccant dehumidification system to handle the latent load and improve the energy efficiency. The energy saving, compared with a conventional vapor compression system, was in the range of 25–50%. The higher the portion of latent load in the total ventilation load was, the more the energy saving was. Gasparella et al. [96] investigated the synergies provided by the combination of an underground thermal energy storage (UTES) system with a desiccant based air handling unit (AHU). Differently from the conventional solutions, the summer humidity control was obtained by chemical dehumidification of the ventilation air stream performed by liquid desiccants in a packed column. The described solution was investigated by a computer simulation referring to a modern office building in the climate of northern Italy. The performance was compared to a traditional HVAC plant and to a traditional ground source heat pump system. Further, some economic evaluations were reported, showing the competitiveness of the proposed configuration.

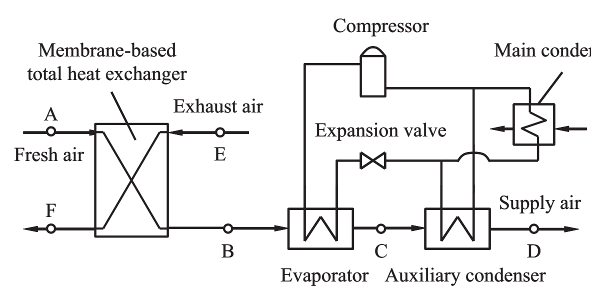


Fig. 10. Schematic of an independent air dehumidification with membrane-based total heat recovery [97,98].

In view of the benefits of the combinations of the liquid desiccant air dehumidification system and other air-conditioning devices [92–96], Zhang and Liang [97,98] proposed and built a fresh air refrigeration dehumidification system with membrane total heat exchanger. The schematic for this system was shown in Fig. 10. This system was relatively simple, since the membrane system had no moving parts, and was compact. The system comprised of all the necessary parts for real application. The theory was that in this system, a membrane based total heat exchanger was used before the fresh air

was pumped to a heat pump for air dehumidification. The total heat exchanger had a membrane core where the incoming fresh air exchanged heat and moisture simultaneously with the exhaust air. In this manner, the total heat or enthalpy from the exhaust was recovered. The mechanical refrigeration system was suitable to use in densely populated urban regions like Guangzhou city. A detailed mathematic model based on cell-by-cell approach was developed to optimize the system [97,98]. Experiments were conducted to validate the model. Then the effects of operating conditions on the dehumidification capacity and the coefficient of performance were investigated. The results helped to optimize the demonstrative unit.

Similarly, Zhang and Huang [68–71] proposed a membrane liquid desiccant air dehumidification system driven by a heat pump, as shown in Fig. 11. As seen, there existed two flowing cycles, namely, the refrigerant cycle in compressor, condenser, expansion valve and evaporator, and the liquid desiccant cycle in dehumidifier, condenser, regenerator and evaporator. The benefits of this system were: (1) The liquid desiccant solution to the regenerator was heated by the condenser directly, and the solution to the dehumidifier was cooled by the evaporator directly. Heat exchange effectiveness was high due to the direct heating and cooling driven by the heat pump. (2) The traditional dehumidifier and regenerator, packed beds, were replaced by the membrane contactors. There were two cross-flow hollow fiber membrane contactors, one for air dehumidification and the other for solution regeneration. Structures of the two contactors were the same. The evaporator and the condenser were made with stainless steel to prevent corrosion.

More recently, Zhang and Huang [99] presented a membrane-based liquid dehumidification system combining with a total heat exchanger, as shown in Fig. 12. As seen, generally, it was similar to the device depicted in Fig. 11. However there were two distinct differences between them. One was that the liquid solution out of the regenerator was pre-cooled by the solution out of the dehumidifier through a plate-type heat exchanger. The other one was that heat and moisture were exchanged between the fresh air and indoor exhaust air in a total heat exchanger. Then the fresh air was sent into the dehumidifier. The total heat of the exhaust air could be recovered and the fresh air could be pre-refrigerated. Compared to the membrane-based liquid desiccant air dehumidification system shown in Fig. 11, the COP of the air dehumidification system shown in Fig. 12, was higher.

The liquid desiccant air dehumidification systems presented in [68–71,92–99] were single-stage air dehumidification systems. Although the desiccant solution was cooled before it was pumped into the dehumidifier, the increase in solution temperature, due to

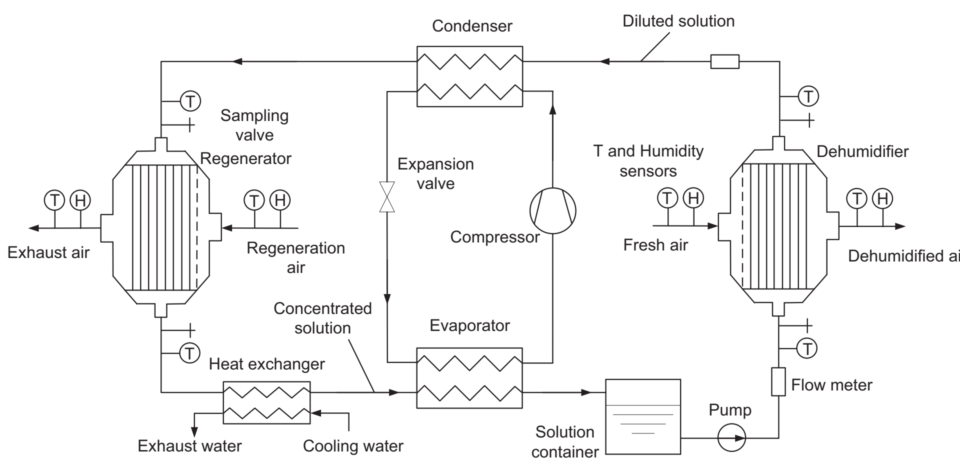


Fig. 11. The membrane-based liquid desiccant air dehumidification system driven by a heat pump [68–71].

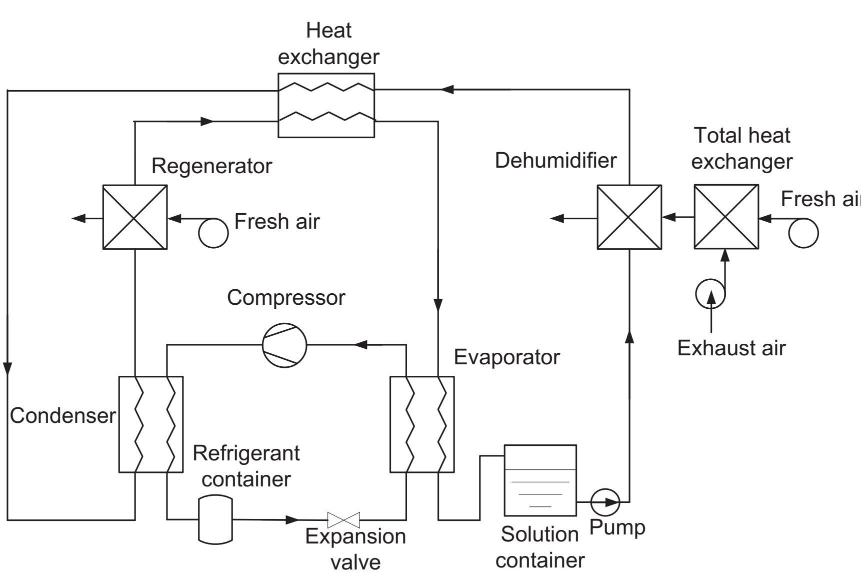


Fig. 12. The membrane-based liquid desiccant air dehumidification system combining with a total heat exchanger [99].

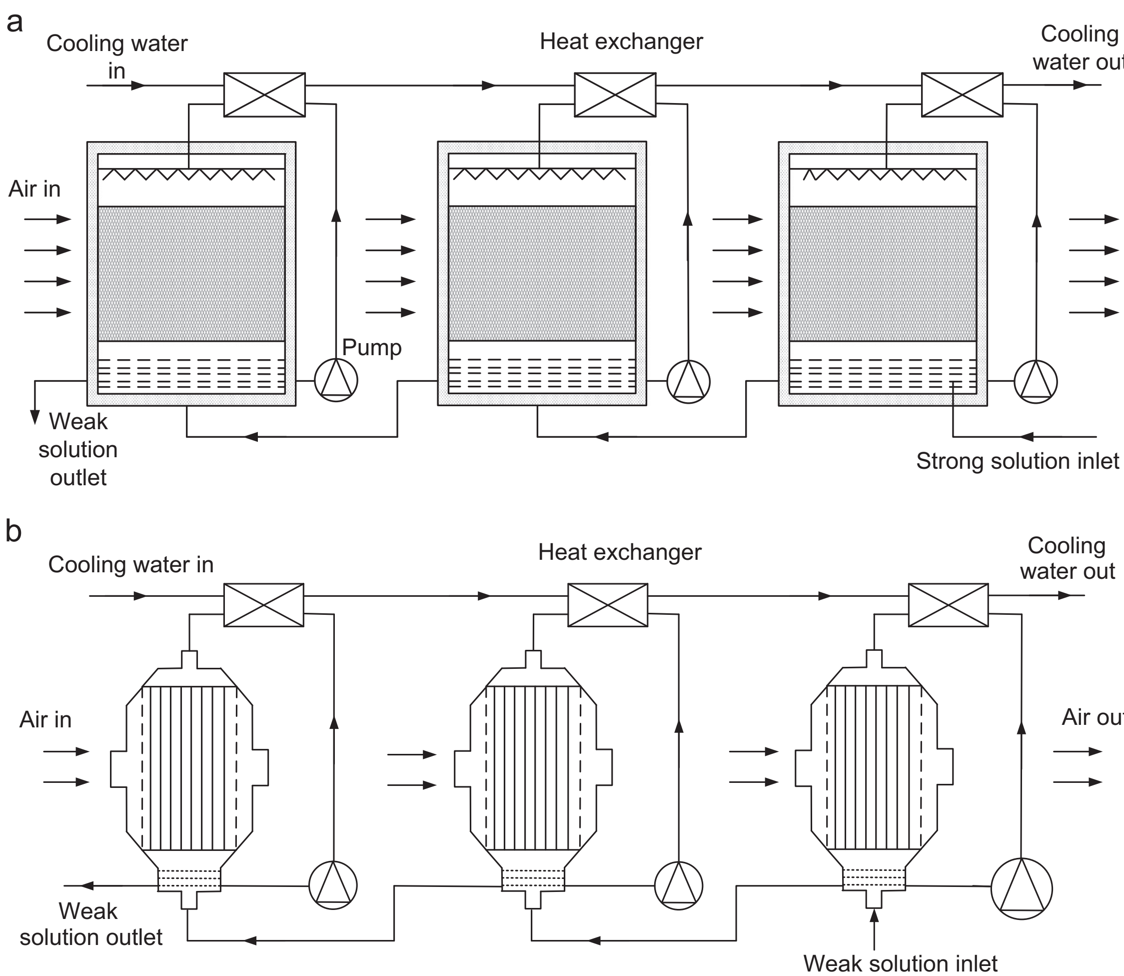


Fig. 13. Schematic diagram of the multi-stage dehumidifier [101]. (a) Packing column type dehumidifier; (b) hollow fiber membrane module type dehumidifier.

moisture removal, was inevitable. For single-stage dehumidification system, an adverse temperature increase in desiccant solution, which would lower the driving force for mass transfer between desiccant solution and process air, would be resulted. Xiong et al. [100] studied a two-stage solar powered liquid–desiccant dehumidification system. It was found that the pre-dehumidification effect of $CaCl_2$ solution was significant in high ambient humidity condition. Also seen was that the desiccant investment could be decreased by 53%, and the Tcop and COP of the system could reach 0.97 and 2.13, respectively. Jiang et al. [101] presented a multi-stage dehumidifier, as shown in Fig. 13(a), which introduced an original dehumidifier by installing several single dehumidifier modules in series. The liquid desiccant flowed from module to module and was separately cooled in every single dehumidifier module to realize better dehumidification. This new mode of dehumidification overcame the potential disadvantage in the conventional single-stage dehumidification. Considering the benefits of the multi-stage air dehumidifier, the membrane-based liquid desiccant air dehumidifier could be extended to be a multi-stage one, as shown in Fig. 13(b).

5. Conclusions and perspectives

It had been observed that the membrane-based liquid desiccant air dehumidification technology was an effective method to solve the problem of liquid desiccant droplets cross-over encountered in the traditional air–liquid directly contacting dehumidifier. The membrane materials, structures of packing column and membrane-based dehumidifiers, the heat and mass transport behaviors in membrane modules, and the applications of new liquid desiccant air dehumidification systems were reviewed in this paper. Following results can be found:

(1) The risks for leakage in the liquid desiccant air dehumidification process were overcome by using nonporous membranes.
(2) The fundamental data obtained by recent works were useful for future membrane module design and system optimum. Installation of the cooling coil in the adiabatic membrane module to form an internally cooled membrane-based dehumidifier may be a sound alternative.
(3) It was obvious that the combinations of the membrane liquid desiccant air dehumidification system with other air-conditioning equipments provided better performance. Further, the authors believed that the multi-stage membrane liquid desiccant air dehumidification system would be the future trend of development.

Acknowledgments

The project is supported by National Natural Science Foundation of China, Nos. 51076047 and 51161160562.

References

[1] Zhang LZ. Total heat recovery: heat and moisture recovery from ventilation air.New York: Nova Science Publishers Inc; 2008.

[2] Grossman G. Solar cooling, dehumidification, and air-conditioning. Encyclopedia of Energy 2004:575–85.
[3] Zhang XR, Zhang LZ, Liu HM, Pei LX. One-step fabrication and analysis of an asymmetric cellulose acetate membrane for heat and moisture recovery. Journal of Membrane Science 2011;366(1–2):158–65.
[4] Zhang LZ. Progress on heat and moisture recovery with membranes: form fundamentals to engineering applications. Energy Conservation and Management 2012;63:173–95.
[5] Zhang LZ, Wang YY, Wang CL, Xiang H. Synthesis and characterization of a PVA/LiCl blend mem brane for air dehumidification. Journal of Membrane Science 2008;308(1–2):198–206.
[6] Liu HM. Preparation and hydrophobic modification of polyvinylidene fluoride.Guangzhou: South China University of Technology; 2011 ([in Chinese]).
[7] Gabelmann A, Hwang ST. Hollow fiber membrane contactors. Journal of Membrane Science 1999;159(1):61–106.
[8] Jansen AE, Feron PHM. Method for gas absorption across a membrane. US Patent no. 5749941; 1998.
[9] Dindore VY, Brilman DWF, Feron PHM, Versteeg GF. CO_2 absorption at elevated pressures using a hollow fiber membrane contactor. Journal of Membrane Science 2004;235(1–2):99–109.
[10] Ter Meulen BP. Method and device for regulating the humidity of a gas flow and at the same time purifying it of undesired acid or alkaline gasses. WO Patent no. 011204; 1994.
[11] Woods J, Pellegrino J, Kozubal E, Slayzak S, Burch J. Modeling of a membrane-based absorption heat pump. Journal of Membrane Science 2009;337(9):113–24.
[12] Sirkar KK, Majumdar SM, Poddar T. Apparatus for removal of volatile organic compounds from gaseous mixtures. US Patent no. 6165253; 2000.
[13] Li K, Teo WK. An ultrathin skinned hollow fibre module for gas absorption at elevated pressures. Chemical Engineering Research & Design 1996;74(8):856–62.
[14] Lee Y, Noble RD, Yeom BY, Park YI, Lee KH. Analysis of CO_2 removal by hollow fiber membrane contactors. Journal of Membrane Science 2001;194(1):57–67.
[15] Witzko R, Bier C. Gas absorption mit Membrankontaktoren. German Patent no. 19639965; 1998.
[16] Zurigat YH, Abu-Arabi MK, Abdul-Wahab SA. Air dehumidification by triethylene glycol desiccant in a packed column. Energy Conversion and Management 2004;45(1):141–55.
[17] Chung TW. Predictions of moisture removal efficiencies for packed-bed dehumidification systems. Gas Separation and Purification 1994;8(4):265–8.
[18] Martin V, Goswami DY. Effectiveness of heat and mass transfer processes in a packed bed liquid desiccant dehumidifier/regenerator. HVAC&R Research 2000;6(1):21–39.
[19] Babakhani D, Soleymani M. An analytical solution for air dehumidification by liquid desiccant in a packed column. International Communications in Heat and Mass Transfer 2009;36(9):969–77.
[20] Moon CG, Bansal PK, Jain S. New mass transfer performance data of a cross-flow liquid desiccant dehumidification system. International Journal of Refrigeration 2009;2(3):524–33.
[21] Zhang L, Hihara E, Matsuoka F. Experimental analysis of mass transfer in adiabatic structured packing dehumidifier/regenerator with liquid desiccant. International Journal of Heat and Mass Transfer 2010;53(13–14):2856–63.
[22] Gao WZ, Liu JH, Cheng YP, Zhang XL. Experimental investigation on the heat and mass transfer between air and liquid desiccant in a cross-flow dehumidifier. Renewable Energy 2012;37:117–23.
[23] Longo GA, Gasparella A. Experimental analysis on chemical dehumidification of air by liquid desiccant and desiccant regeneration in a packed tower. Journal of Solar Energy Engineering—Transactions of the ASME 2004;126(1):587–91.
[24] Yoon JI, Phan TT, Moon CG, Bansal P. Numerical study on heat and mass transfer characteristic of plate absorber. Applied Thermal Engineering 2005;25(14–15):2219–35.
[25] Khan AY, Sulsona FJ. Modeling and parametric analysis of heat and mass transfer performance of refrigerant and cooled liquid desiccant absorbers. International Journal of Energy Research 1998;22(9):813–32.
[26] Saman WY, Alizadeh S. An experimental study of a cross-flow type plate heat exchanger for dehumidification/cooling. Solar Energy 2002;73(1):59–71.
[27] Liu XH, Chang XM, Xia JJ, Jiang Y. Performance analysis on the internally cooled dehumidifier using liquid desiccant. Building and Environment 2009;44(2):299–308.
[28] Yin YG, Zhang XS, Peng DG, Li XW. Model validation and case study on internally cooled/heated dehumidifier/regenerator of liquid desiccant systems. International Journal of Thermal Sciences 2009;48(8):1664–71.
[29] Zhang LZ. Heat and mass transfer in a cross-flow membrane-based enthalpy exchanger under naturally formed boundary conditions. International Journal of Heat and Mass Transfer 2007;50(1–2):151–62.
[30] Zhang LZ, Liang CH, Pei LX. Conjugate heat and mass transfer in membrane-formed channels in all entry regions. International Journal of Heat and Mass Transfer 2010;53(5–6):815–24.
[31] Mahmud K, Mahmood GI, Simonson CJ, Besant RW. Performance testing of a counter-cross- flow run-around membrane energy exchanger (RAMEE) system for HVAC applications. Energy and Buildings 2010;42(7):1139–47.
[32] Vali A, Simonson CJ, Besant RW, Mahmood G. Numerical model and effectiveness correlations for a run-around heat recovery system with combined counter and cross flow exchangers. International Journal of Heat and Mass Transfer 2009;52(25–26):5827–40.
[33] Larson MD, Simonson CJ, Besan RW. The elastic and moisture transfer properties of polyethylene and polypropylene membranes for use in liquid-to-air energy exchangers. Journal of Membrane Science 2007;302(1–2):136–49.
[34] Seyed-Ahmadi M, Erb B, Simonson CJ, Besant RW. Transient behavior of run-around heat and moistu- re exchanger system. Part I: Model formulation and verification. International Journal of Heat and Mass Transfer 2009;52(1–2):6000–11.
[35] Seyed-Ahmadi M, Erb B, Simonson CJ, Besant RW. Transient behavior of run-around heat and moisture exchanger system. Part II: Sensitivity studies for a range of initial conditions. International Journal of Heat and Mass Transfer 2009;52(25–26):6012–20.
[36] Li JL, Ito A. Dehumidification and humidification of air by surface-soaked liquid membrane module with triethylene glycol. Journal of Membrane Science 2008;325(2):1007–12.
[37] Huang SM, Zhang LZ, Tang K, Pei LX. Fluid flow and heat mass transfer in membrane parallel-plates channels used for liquid desiccant air dehumidification. International journal of heat and mass transfer 2012;55(9–10):2571–80.
[38] Incropera FP, Dewitt DP. Introduction to heat transfer. 3th ed.New York: John Wiley & Sons publishers Inc; 1996.
[39] Holman JP. Heat transfer. 9th ed.New York: McGraw-Hill; 2005.
[40] Mansourizadeh A, Ismail AF. Hollow fiber gas–liquid membrane contactors for acid gas capture: a review. Journal of Hazardous Materials 2009;171(1–3):38–53.
[41] Zhang HY, Wang R, Liang DT, Tay JH. Modeling and experimental study of CO_2 absorption in a hollow fiber membrane contactor. Journal of Membrane Science 2006;279(1–2):301–10.
[42] Keshavarz P, Fathikalajahi J, Ayatollahi S. Analysis of CO_2 separation and simulation of a partially wetted hollow fiber membrane contactor. Journal of Hazardous Materials 2008;152(3):1237–47.
[43] Gong Y, Wang Z, Wang S. Experiments and simulation of CO_2 removal by mixed amines in a hollow fiber membrane module. Chemical Engineering and Processing 2006;45(8):652–60.
[44] Zhang LZ, Huang SM. Coupled heat and mass transfer in a counter flow hollow fiber membrane module for air humidification. International Journal of Heat and Mass Transfer 2011;54(5–6):1055–63.
[45] Cussler EL. Diffusion–mass transfer in fluid systems.Cambridge: Cambridge University Press; 2000.
[46] Leveque MA. Les lois de la transmission de chaleur par convection. Annual Mines 1928;13:201–99.
[47] Graetz L. Uber die Warmeleitungsfahigkeit von Flussigkeiten. Annalen der Physik und Chemie 1885;25:337–57.
[48] Kreulen H, Smolders CA, Versteeg GF, Swaaij WPMV. Microporous hollow fiber membrane modules as gas–liquid contactors. Part 1. Physical mass transfer processes: a specific application: mass transfer in highly viscous liquids. Journal of Membrane Science 1993;78(3):197–216.
[49] Happel J. Viscous flow relative to arrays of cylinders. AIChE Journal 1959;5:174–7.
[50] Mavroudi M, Kaldis SP, Sakellaropoulos GP. Reduction of CO_2 emissions by a membrane contacting process. Fuel 2003;82(15–17):2153–9.
[51] Mavroudi M, Kaldis SP, Sakellaropoulos GP. A study of mass transfer resistancein membrane gas–liquid contacting processes. Journal of Membrane Science 2006;272(1–2):103–15.
[52] Li K, Kong J, Tan X. Design of hollow fiber membrane modules for soluble gas removal. Chemical Engineering Science 2000;55(23):5579–88.
[53] Costello MJ, Fane AG, Hogan PA, Schofield RW. The effect of shell-side hydrodynamics on the performance of axial flow hollow fiber modules. Journal of Membrane Science 1993;80(1–2):1–10.
[54] Prasad R, Sirkar KK. Dispersion-free extraction with microporous hollow fibre modules. AIChE Journal 1988;34:177–81.
[55] Zhang LZ. Heat and mass transfer in a randomly packed hollow fiber membrane module: a fractal model approach. International Journal of Heat and Mass Transfer 2011;54(13–14):2921–31.
[56] Yang MC, Cussler EL. Designing hollow-fiber contactors. AIChE Journal 1986;32:1910–6.
[57] Wu J, Chen V. Shell-side mass transfer performance of randomly packed hollow fiber modules. Journal of Membrane Science 2000;172(1–2):59–74.
[58] Cote P, Bersillon JL, Huyard A. Bubble-free aeration using membranes: mass transfer analysis. Journal of Membrane Science 1989;47:91–106.
[59] Zheng JM, Xu YY, Xu ZK. Shell side mass transfer characteristics in a parallel flow hollow fiber membrane module. Separation Science and Technology 2003;38(1–2):1247–67.
[60] Nii S, Takeuchi H. Removal of CO_2 and/or SO_2 from gas streams by a membrane absorption method. Gas Separation and Purification 1994;8(2):107–16.
[61] Lipnizki F, Field RW. Mass transfer performance for hollow fiber modules with shell-side axial feed flow using engineering approach to develop a framework. Journal of Membrane Science 2001;193(1–2):195–208.
[62] Zhang LZ, Huang SM, Tang K, Pei LX. Conjugate heat and mass transfer in a hollow fiber membrane module for liquid desiccant air dehumidification: a free surface model approach. International Journal of Heat and Mass Transfer 2012;55(13–14):3789–99.
[63] Bergero S, Chiari A. Experimental and theoretical analysis of air humidification/dehumidifycation processes using hydrophobic capillary contactors. Applied Thermal Engineering 2001;21(11):1119–35.

[64] Kneifel K, Nowak S, Albrecht W, Hike R, Just R, Peinemann KV. Hollow fiber membrane contactor for air humidity control. Journal of Membrane Science 2006;276(2):241–51.
[65] Johnson D, Yavuzturk WC, Pruis J. Analysis of heat and mass transfer phenomena in hollow fiber membranes used for evaporative cooling. Journal of Membrane Science 2003;227(1–2):159–71.
[66] Dijkink BH, Tomassen MM, Willemsen JHA, Doorn WGV. Humidity control during bell pepper storage, using a hollow fiber membrane contactor system. Postharvest Biology and Technology 2004;32(3):311–20.
[67] Isetti C, Nannei E, Magrini A. On the application of a membrane air–liquid contactor for air dehumidification. Energy and Building 1997;25(3):185–93.
[68] Zhang LZ, Huang SM, Pei LX. Conjugate heat and mass transfer in a cross-flow hollow fiber membrane contactor for liquid desiccant air dehumidification. International journal of heat and mass transfer 2013;55(25–26):8061–72.
[69] Huang SM, Zhang LZ, Tang K, Pei LX. Turbulent heat and mass transfer across a hollow fiber membrane module in liquid desiccant air dehumidification. ASME Journal of Heat Transfer 2012;134(8):082001-1–10.
[70] Huang SM, Zhang LZ, Pei LX. Transport phenomena in a cross-flow hollow fiber membrane bundle used for liquid desiccant air dehumidification. Indoor and Built Environment 2013;22(3):559–74.
[71] Zhang LZ, Huang SM, Zhang WB. Turbulent heat and mass transfer across a hollow fiber membrane bundle considering interactions between neighboring fibers. International Journal of Heat and Mass Transfer 2013;64:162–72.
[72] Dhotkar BN, Chhabra RP, Eswaran V. Flow of non-Newtonian polymeric solutions in fibrous media. Journal of Applied Polymer Science 2000;76(7):1171–85.
[73] Chhabra RP, Dhotkar BN, Eswaran V, Satheesh VK, Vijaysri M. Steady flow of Newtonian and dilatants fluids over an array of long circular cylinders. Journal of Chemical Engineering of Japan 2000;33(6):832–41.
[74] Shibu S, Chhabra RP, Eswaran V. Power law fluid flow over a bundle of cylinders at intermediate Reynolds numbers. Chemical Engineering Science 2000;56(19):5545–54.
[75] Vijaysri M, Chhabra RP, Eswaran V. Power law fluid flow across an array of in6nite circular cylinders: a numerical study. Journal of Non-Newtonian Fluid Mechanics 1999;87(2–3):263–82.
[76] Satheesh VK, Chhabra RP, Eswaran V. Steady incompressible fluid flow over a bundle of cylinders at moderate Reynolds numbers. Canadian Journal of Chemical Engineering 1999;77(5):978–87.
[77] Mandhani VK, Chhabraa RP, Eswaran V. Forced convection heat transfer in tube banks in cross flow. Chemical Engineering Science 2002;57(3):379–91.
[78] Chen CJ, Wung TS. Finite analytic solution of convective heat transfer for tube arrays in cross flow: Part II—heat transfer analysis. ASME Journal of Heat Transfer 1989;111(3):641–8.
[79] Wung TS, Chen CJ. Finite analytic solution of convective heat transfer for tube arrays in cross flow: Part I—flow field analysis. ASME Journal of Heat Transfer 1989;111(3):633–40.
[80] Martin AR, Saltiel C, Shyy W. Frictional losses and convective heat transfer in sparse, periodic cylinder arrays in cross flow. International Journal of Heat Mass Transfer 1998;41:2383–97.
[81] Wilson AS, Bassiouny MK. Modeling of heat transfer for flow across tube banks. Chemical Engineering and Processing 2000;39(1):1–14.
[82] Yoo SY, Kwonb HK, Kim JH. A study on heat transfer characteristics for staggered tube banks in cross-flow. Journal of Mechanical Science and Technology 2007;21(3):505–12.
[83] Kim MS, Baek BJ, Pak BC. An experimental study of fouling effect on the heat transfer around a tube in staggered tube banks. Transactions of the Korean Society of Mechanical Engineers 2000;24(11):1478–85.
[84] Buyruk E. Numerical study of heat transfer characteristics on tandem cylinders, inline and staggered tube banks in cross-flow of air. International journal of Communications in Heat and Mass Transfer 2002;29:355–66.
[85] Lange CF, Durst F, Breuer M. Momentum and heat transfer from cylinders in laminar cross flow at $10^{-4} < Re < 2000$. International Journal of Heat Mass Transfer 1998;41(22):3409–30.
[86] Colburn AP. A method of correlating forced convection heat transfer data and a comparison with fluid friction. Transactions of American Institute of Chemical Engineers 1993;29:174–210.
[87] Huge EC. Experimental investigation of effects of equipment size on convection heat transfer and flow resistance in cross flow of gases over tube banks. Journal of Dynamic Systems, Measurement and Control, Series G 1937;59:573–81.
[88] Pierson OL. Experimental investigation of the influence of tube arrangement on convection heat transfer and flow resistance in cross flow of gases over tube banks. Journal of Dynamic Systems, Measurement and Control, Series G 1937;59:563–72.
[89] Grimison ED. Correlation and utilization of new data on flow resistance and heat transfer for cross flow of gases over tube banks. Journal of Dynamic Systems, Measurement and Control, Series G 1937;59:583–94.
[90] Zukauskas A. Heat transfer from tubes in cross-flow. Advances in Heat Transfer 1972;8:93–160.
[91] Hausen H. Heat transfer in counter flow, parallel flow and cross flow.New York: McGraw-Hill; 1983.
[92] Xiao F, Ge GM, Niu XF. Control performance of a dedicated outdoor air system adopting liquid desiccant dehumidification. Applied Energy 2011;88(1):143–9.
[93] Nayak SM, Hwang Y, Radermacher R. Performance characterization of gas engine generator integrated with a liquid desiccant dehumidification system. Applied Thermal Engineering 2009;29(2–3):479–90.
[94] Sayegh MA, Hammad M, Faraa Z. Comparison of two methods of improving dehumidification in air conditioning systems: hybrid system (refrigeration cycle-rotary desiccant) and heat exchanger cycle. Energy Procedia 2011;6:759–68.
[95] Li YT, Yang HX. Investigation on solar desiccant dehumidification process for energy conservation of central air-conditioning systems. Applied Thermal Engineering 2008;28(10):1118–26.
[96] Gasparella A, Longo GA, Marra R. Combination of ground source heat pumps with chemical dehumidification of air. Applied Thermal Engineering 2005;25(2):295–308.
[97] Liang CH, Zhang LZ, Pei LX. Independent air dehumidification with membrane-based total heat recovery: modeling and experimental validation. International Journal of Refrigeration 2010;33(2):398–408.
[98] Liang CH, Zhang LZ, Pei LX. Performance analysis of a direct expansion air dehumidification system combined with membrane-based total heat recovery. Energy 2010;35(9):3891–901.
[99] Zhang LZ, Huang SM, Pei LX. A membrane-based liquid desiccant air dehumidification and energy storage device driven by a heat pump. Chinese Patent, ZL 201020541934, 2010.
[100] Xiong ZQ, Dai YJ, Wang RZ. Investigation on a two-stage solar liquid–desiccant (LiBr) dehumidification system assisted by $CaCl_2$ solution. Applied Thermal Engineering 2009;29(5–6):1209–15.
[101] Jiang Y, Li Z, Chen XL, Liu XH. Liquid desiccant air conditioning system and its applications. Heat Ventilation Air Condition 2004;34(11):88–98.